

Advection of nematic liquid crystals by chaotic flow

Lennon Ó Náraigh

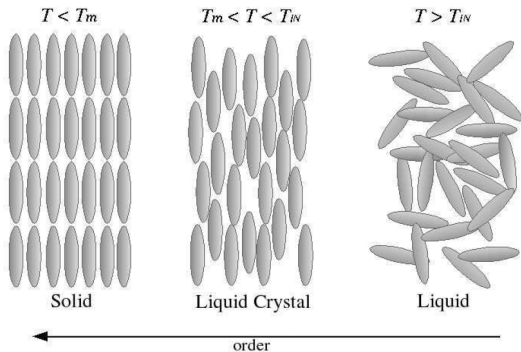
Home fixture

21st September 2016

Context of work

Liquid crystals are rodlike molecules that possess an intermediate phase between solid and liquid, hence two melting points:

- An upper melting point T_m : the substance is in a solid phase for $T < T_m$
- A lower melting point T_{IN} : the substance behaves like an isotropic liquid for $T > T_{IN}$.

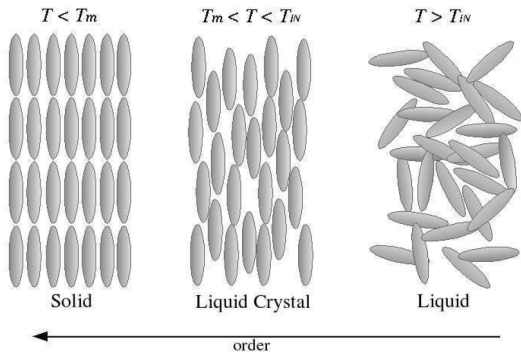


Context of work

Liquid crystals are rodlike molecules that possess an intermediate phase between solid and liquid, hence two melting points:

- An upper melting point T_m : the substance is in a solid phase for $T < T_m$
- A lower melting point T_{IN} : the substance behaves like an isotropic liquid for $T > T_{IN}$.

Between these values, the substance has orientational order and behaves like a fluid with a highly complicated rheology – a **liquid crystal**.



Applications

Liquid crystals aligned in a single direction have the same optical properties as uniaxial crystals, yet their properties are easily modified by outside influences (e.g. electrical fields, strain fields, etc.), hence their ubiquity in LCDs.



Another way to modify liquid crystal properties – **hydrodynamics** – the main focus of this talk.

Modelling Approach

The **director** $\hat{\mathbf{n}}(\mathbf{x}, t)$ gives the mesoscopically-averaged direction of molecular orientation at a point \mathbf{x} . We need to formulate evolution equations for $\hat{\mathbf{n}}(\mathbf{x}, t)$.

Molecules have head-tail symmetry, so it's better to formulate the equations in terms of a symmetric, traceless **Q-tensor**, where

$$Q_{ij} = (2\lambda_1 + \lambda_2) \left(n_i^{(1)} n_j^{(2)} - \frac{1}{3} \delta_{ij} \right) + (2\lambda_2 + \lambda_1) \left(n_i^{(2)} n_j^{(2)} - \frac{1}{3} \delta_{ij} \right).$$

If $2\lambda_2 + \lambda_1 = 0$ then the Q-tensor has a 'familiar' form,

$$Q_{ij} = \frac{1}{2} S \left(n_i^{(1)} n_j^{(2)} - \frac{1}{3} \delta_{ij} \right), \quad S = 3\lambda_1 \text{ (scalar **order parameter**)}$$

and the eigenvector can be unambiguously identified with the direction of the (ahem) director – rodlike molecule – **uniaxial case**.

For the general case, there are three directions associated with the Q-tensor – ellipsoidal molecule (**biaxial** liquid crystal)

Landau theory

We apply Landau theory to the system near the liquid/liquid-crystal transition temperature, writing the free energy of the system as

$$F = F_0 + F_K,$$

where F_0 is the double-well part associated with the phase change:

$$F_0 = \int d^3x \chi(\mathbf{Q}), \quad \chi(\mathbf{Q}) = \frac{1}{2} \alpha_F \text{tr}(\mathbf{Q}^2) - \beta_F \text{tr}(\mathbf{Q}^3) + \gamma_F [\text{tr}(\mathbf{Q}^2)]^2,$$
$$\alpha_F = 12a(T - T_*).$$

The term F_K is the energy penalty for distortions,

$$F_K = \int d^3x W(\nabla \mathbf{Q}), \quad W(\nabla \mathbf{Q}) = \frac{1}{2} k \|\nabla \mathbf{Q}\|_2^2$$

under the one-elastic-constant assumption (bend, splay, and twist all energetically equally unfavourable).

Structure of quartic potential, uni-axial case

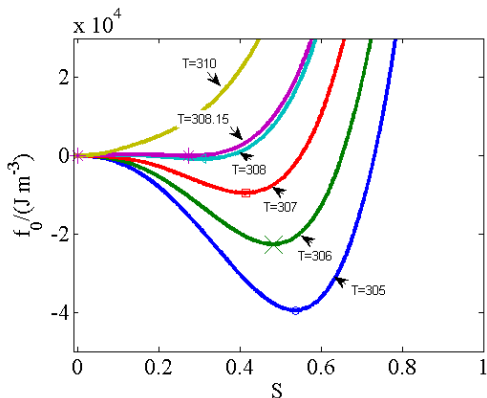
In the absence of inhomogeneities, we can understand the structure of the quartic potential $\chi(\mathbf{Q})$, using

$$\chi(S) = \frac{1}{12}\alpha_F S^2 - \underbrace{\frac{1}{36}\beta_F}_{=B} S^3 + \underbrace{\frac{1}{36}\gamma_F}_{=C} S^3, \quad S = \sqrt{6 \operatorname{tr}(\mathbf{Q}^2)}, \quad Q_{ij} \text{ uniaxial}$$

- Free-energy minima
 $(\partial\chi/\partial S)_{S_*} = 0$
- Nematic state favourable compared to isotropic one:
 $\chi(S_*, T) > \chi(0, T)$
- Gives critical temperature

$$T_{IN} = T_* + \frac{B^2}{4ac},$$

where $\alpha_F = 12a(T - T_*)$.



Gradient dynamics

With inhomogeneities present, but without flow, system evolves so as to minimize its free energy – subject to the constraint (Lagrange multiplier) that the Q -tensor remains traceless. Result –

$$\zeta_1 \frac{\partial Q_{ij}}{\partial t} = - \left[\frac{\delta F}{\delta Q_{ij}} - \frac{1}{3} \text{tr} \left(\frac{\delta F}{\delta Q_{ij}} \right) \delta_{ij} \right].$$

Coupling to incompressible flow – continuum mechanics I

- Write down Lagrangian for incompressible flow, constant density ρ_0 :

$$L = \int_{\Omega} d^3a \left\{ \frac{1}{2} \left(\frac{\partial \mathbf{x}}{\partial t} \right)^2 + \left(1 - \frac{\rho}{\rho_0} \right) \frac{p}{\rho_0} \right\} - \int_{\Omega} \frac{d^3a}{\rho_0} [\chi(\mathbf{Q}) + W(\mathbf{Q}) - \lambda \mathbf{Q} \cdot \mathbb{I}]$$

where \mathbf{a} is a particle label and $\rho_0 d^3x = d^3a$.

Coupling to incompressible flow – continuum mechanics I

- Write down Lagrangian for incompressible flow, constant density ρ_0 :

$$L = \int_{\Omega} d^3a \left\{ \frac{1}{2} \left(\frac{\partial \mathbf{x}}{\partial t} \right)^2 + \left(1 - \frac{\rho}{\rho_0} \right) \frac{p}{\rho_0} \right\} - \int_{\Omega} \frac{d^3a}{\rho_0} [\chi(\mathbf{Q}) + W(\mathbf{Q}) - \lambda \mathbf{Q} \cdot \mathbb{I}]$$

where \mathbf{a} is a particle label and $\rho_0 d^3x = d^3a$.

- The generalized forces are

$$\mathbf{F}_{\mathbf{v}} = \frac{\partial}{\partial \tau} \frac{\delta L}{\delta(\partial \mathbf{x} / \partial \tau)} - \frac{\delta L}{\delta \mathbf{x}}, \quad \mathbf{F}_{\mathbf{Q}} = \frac{\partial}{\partial \tau} \frac{\delta L}{\delta(\partial \mathbf{Q} / \partial \tau)} - \frac{\delta L}{\delta \mathbf{Q}},$$

where $\mathbf{v} = \partial \mathbf{x} / \partial \tau$ is the velocity of a Lagrangian particle.

Coupling to incompressible flow – continuum mechanics I

- Write down Lagrangian for incompressible flow, constant density ρ_0 :

$$L = \int_{\Omega} d^3a \left\{ \frac{1}{2} \left(\frac{\partial \mathbf{x}}{\partial t} \right)^2 + \left(1 - \frac{\rho}{\rho_0} \right) \frac{p}{\rho_0} \right\} - \int_{\Omega} \frac{d^3a}{\rho_0} [\chi(\mathbf{Q}) + W(\mathbf{Q}) - \lambda \mathbf{Q} \cdot \mathbb{I}]$$

where \mathbf{a} is a particle label and $\rho_0 d^3x = d^3a$.

- The generalized forces are

$$\mathbf{F}_{\mathbf{v}} = \frac{\partial}{\partial \tau} \frac{\delta L}{\delta(\partial \mathbf{x} / \partial \tau)} - \frac{\delta L}{\delta \mathbf{x}}, \quad \mathbf{F}_{\mathbf{Q}} = \frac{\partial}{\partial \tau} \frac{\delta L}{\delta(\partial \mathbf{Q} / \partial \tau)} - \frac{\delta L}{\delta \mathbf{Q}},$$

where $\mathbf{v} = \partial \mathbf{x} / \partial \tau$ is the velocity of a Lagrangian particle.

- Dissipation is accounted for by dissipative forces; these are $-\delta \mathcal{R} / \delta \mathbf{v}$ and $-\delta \mathcal{R} / \delta \mathbf{Q}$, where \mathcal{R} is a dissipative function, to be modelled.

Coupling to incompressible flow – continuum mechanics I

- Write down Lagrangian for incompressible flow, constant density ρ_0 :

$$L = \int_{\Omega} d^3a \left\{ \frac{1}{2} \left(\frac{\partial \mathbf{x}}{\partial t} \right)^2 + \left(1 - \frac{\rho}{\rho_0} \right) \frac{p}{\rho_0} \right\} - \int_{\Omega} \frac{d^3a}{\rho_0} [\chi(\mathbf{Q}) + W(\mathbf{Q}) - \lambda \mathbf{Q} \cdot \mathbb{I}]$$

where \mathbf{a} is a particle label and $\rho_0 d^3x = d^3a$.

- The generalized forces are

$$\mathbf{F}_{\mathbf{v}} = \frac{\partial}{\partial \tau} \frac{\delta L}{\delta(\partial \mathbf{x} / \partial \tau)} - \frac{\delta L}{\delta \mathbf{x}}, \quad \mathbf{F}_{\mathbf{Q}} = \frac{\partial}{\partial \tau} \frac{\delta L}{\delta(\partial \mathbf{Q} / \partial \tau)} - \frac{\delta L}{\delta \mathbf{Q}},$$

where $\mathbf{v} = \partial \mathbf{x} / \partial \tau$ is the velocity of a Lagrangian particle.

- Dissipation is accounted for by dissipative forces; these are $-\delta \mathcal{R} / \delta \mathbf{v}$ and $-\delta \mathcal{R} / \delta \mathbf{Q}$, where \mathcal{R} is a dissipative function, to be modelled.
- Theory is closed by equating dissipative forces with generalized forces:

$$\frac{\partial}{\partial \tau} \frac{\delta L}{\delta(\partial \mathbf{x} / \partial \tau)} - \frac{\delta L}{\delta \mathbf{x}} = -\frac{\delta \mathcal{R}}{\delta \mathbf{v}} \text{ etc.}$$

Coupling to incompressible flow – continuum mechanics II

Dissipation is modelled so as to be a positive-definite materially frame-indifferent quantity. Also, should reduce to Navier–Stokes when $\mathbf{Q} \rightarrow 0$. Hence,

$$\mathcal{R} = \frac{1}{\rho_0} \int_{\Omega} d^3a R,$$

where R is a quadratic function of \mathbf{D} (strain rate) and the **co-rotational derivative**

$$\overset{\circ}{\mathbf{Q}} = \frac{\partial \mathbf{Q}}{\partial t} + \mathbf{v} \cdot \nabla \mathbf{Q} - \boldsymbol{\Omega} \mathbf{Q} + \mathbf{Q} \boldsymbol{\Omega}, \quad \Omega_{ij} = \frac{1}{2} (\partial_i u_j - \partial_j u_i),$$

hence

$$R = R(\mathbf{D}, \mathbf{Q}, \overset{\circ}{\mathbf{Q}}).$$

Final version of equations

Putting this all together, with

$$R = \frac{1}{2}\zeta_1 = \dot{\mathbf{Q}} \cdot \dot{\mathbf{Q}} + \zeta_2 \mathbf{D} \cdot \dot{\mathbf{Q}} + \frac{1}{2}\zeta_3 \mathbf{D} \cdot \mathbf{D} + \frac{1}{2}\zeta_{31} \mathbf{D} \cdot (\mathbf{D}\mathbf{Q}) + \frac{1}{2}\zeta_{32} (\mathbf{D} \cdot \mathbf{Q})^2,$$
$$\mathbf{D} \cdot \mathbf{Q} = D_{ij}Q_{ij} \text{ etc.}$$

gives a final set of equations:

Final version of equations

Putting this all together, with

$$R = \frac{1}{2}\zeta_1 = \dot{\mathbf{Q}} \cdot \dot{\mathbf{Q}} + \zeta_2 \mathbf{D} \cdot \dot{\mathbf{Q}} + \frac{1}{2}\zeta_3 \mathbf{D} \cdot \mathbf{D} + \frac{1}{2}\zeta_{31} \mathbf{D} \cdot (\mathbf{D}\mathbf{Q}) + \frac{1}{2}\zeta_{32} (\mathbf{D} \cdot \mathbf{Q})^2,$$

$$\mathbf{D} \cdot \mathbf{Q} = D_{ij}Q_{ij} \text{ etc.}$$

gives a final set of equations:

Q-tensor: $\zeta_1 \left(\frac{\partial \mathbf{Q}}{\partial t} + \mathbf{v} \cdot \nabla \mathbf{Q} - \boldsymbol{\Omega} \mathbf{Q} - \mathbf{Q} \boldsymbol{\Omega} \right) + \underbrace{\zeta_2 \mathbf{D}}_{\text{Note inhomogeneity!}} =$

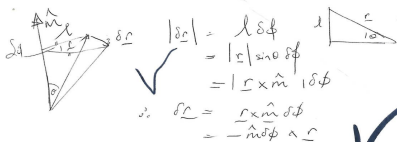
$$k \nabla^2 \mathbf{Q} - (\alpha_F \mathbf{Q} - 3\beta_F \mathbf{Q}^2 + 4\gamma_F \text{tr}(\mathbf{Q}^2) \mathbf{Q}) + \frac{1}{3} \mathbb{I} [\zeta_2 \text{tr}(\mathbf{D}) - 3\beta_F \text{tr}(\mathbf{Q}^2)],$$

Hydrodynamics: $\rho_0 \left(\frac{\partial \mathbf{v}}{\partial t} + \mathbf{v} \cdot \nabla \mathbf{v} \right) = \nabla \cdot \mathbf{T},$

$$\mathbf{T} = -p \mathbb{I} - k \nabla \mathbf{Q} \odot \nabla \mathbf{Q} + \zeta_2 \dot{\mathbf{Q}} + \zeta_3 \mathbf{D} + \zeta_{31} (\mathbf{D}\mathbf{Q} + \mathbf{Q}\mathbf{D}) + \zeta_{32} (\mathbf{D} \cdot \mathbf{Q}) \mathbf{Q},$$

Incompressibility: $\nabla \cdot \mathbf{v} = 0.$

Co-rotational derivative – aside



$$\frac{dr}{dt} = -\hat{m} \frac{d\phi}{dt} \times \hat{r}$$

$$\approx -\hat{m} \Omega \times \hat{r}$$

$$\approx -\underline{\Omega} \times \hat{r}$$

$$\boxed{\frac{dr}{dt} = -\underline{\Omega} \times r}$$

$$\underline{\Omega} = \hat{m} \Omega, \quad \Omega = \frac{d\phi}{dt}$$

$$\frac{dr_i}{dt} = -\epsilon_{i\alpha p} \Omega_\alpha r_p$$

$$\frac{dr_j}{dt} = -\epsilon_{j\alpha p} \Omega_\alpha r_p$$

$$r_i \frac{dr_j}{dt} + r_j \frac{dr_i}{dt} = \frac{d}{dt}(r_i r_j) = -\epsilon_{\alpha p \beta} \Omega_\alpha r_i r_j - \epsilon_{i\alpha p} \Omega_\alpha r_j^2$$

$$Q_{ij} = r_i r_j$$

$$\frac{d}{dt} Q_{ij} = -\epsilon_{i\alpha p} \Omega_\alpha Q_{jp} - \epsilon_{j\alpha p} \Omega_\alpha Q_{ip}$$

$$\Omega_\alpha = \frac{1}{2} (\hat{r} \times \hat{v})_\alpha$$

$$\text{Take } \epsilon_{i\alpha p} \Omega_\alpha Q_{jp} = \frac{1}{2} \epsilon_{i\alpha p} (\epsilon_{\alpha \gamma \delta} \hat{v}_\gamma \hat{v}_\delta) Q_{jp}$$

$$= \frac{1}{2} \epsilon_{i\alpha p} \epsilon_{\alpha \gamma \delta} \hat{v}_\gamma \hat{v}_\delta Q_{jp}$$

$$= -\frac{1}{2} \epsilon_{\alpha p \gamma} \epsilon_{\alpha \delta \gamma} \hat{v}_\delta \hat{v}_\gamma Q_{jp}$$

$$= -\frac{1}{2} (\delta_{i\gamma} \delta_{p\delta} - \delta_{i\delta} \delta_{p\gamma}) \hat{v}_\gamma \hat{v}_\delta \times Q_{jp}$$

$$= -\frac{1}{2} \partial_i v_p Q_{jp} + \frac{1}{2} \partial_p v_i Q_{jp}$$

$$= \frac{1}{2} (\partial_p v_i - \partial_i v_p) Q_{jp}$$

$$W_{pi} = \frac{1}{2} (\partial_p v_i - \partial_i v_p)$$

$$= W_{pi} Q_{jp}$$

$$= -W_{ip} Q_{jp}$$

$$= -(WQ)_{ij}$$



W = antisym.

Q = sym.

$$\therefore \frac{d}{dt} Q_{ij} = -(WQ)_{ij} - (WQ)_{ji}$$

$$= -(WQ)_{ij} - [WQ^T]_{ij}$$

$$= -[a^T W^T]_{ij}$$

$$+ (aW)_{ij}$$

Non-dimensional equations – dimensionless groups

Length scale L and timescale $t_0 = \zeta_1 / (8\gamma_F)$ – hence dimensionless Q-tensor equation

$$\begin{aligned} \frac{\partial \mathbf{Q}}{\partial \tilde{t}} + \tilde{\mathbf{v}} \cdot \tilde{\nabla} \mathbf{Q} - \tilde{\boldsymbol{\Omega}} \mathbf{Q} - \mathbf{Q} \tilde{\boldsymbol{\Omega}} + \underbrace{\text{Tu}}_{=(\zeta_2/\zeta_1)} \tilde{\mathbf{D}} \\ = \epsilon^2 \tilde{\nabla}^2 \mathbf{Q} + g_1(1-\theta) \mathbf{Q} + 3g_2 \mathbf{Q}^2 - \frac{1}{2} \text{tr}(\mathbf{Q}^2) \mathbf{Q} + \frac{1}{3} \mathbb{I} \left[\text{Tu tr}(\tilde{\mathbf{D}}) - 3g_2 \text{tr}(\mathbf{Q}^2) \right], \end{aligned}$$

where

Non-dimensional equations – dimensionless groups

Length scale L and timescale $t_0 = \zeta_1 / (8\gamma_F)$ – hence dimensionless Q-tensor equation

$$\begin{aligned} \frac{\partial \mathbf{Q}}{\partial \tilde{t}} + \tilde{\mathbf{v}} \cdot \tilde{\nabla} \mathbf{Q} - \tilde{\boldsymbol{\Omega}} \mathbf{Q} - \mathbf{Q} \tilde{\boldsymbol{\Omega}} + \underbrace{\mathbf{Tu}}_{=(\zeta_2/\zeta_1)} \tilde{\mathbf{D}} \\ = \epsilon^2 \tilde{\nabla}^2 \mathbf{Q} + g_1(1-\theta) \mathbf{Q} + 3g_2 \mathbf{Q}^2 - \frac{1}{2} \text{tr}(\mathbf{Q}^2) \mathbf{Q} + \frac{1}{3} \mathbb{I} \left[\mathbf{Tu} \text{tr}(\tilde{\mathbf{D}}) - 3g_2 \text{tr}(\mathbf{Q}^2) \right], \end{aligned}$$

where

$$\alpha_F / (8\gamma_F) = -g_1 [1 - (T/T_*)] \equiv -g_1(1-\theta), \quad \beta_F / (8\gamma_F) = g_2, \quad \epsilon = k / (L^2 \gamma_F).$$

Non-dimensional equations – dimensionless groups

Length scale L and timescale $t_0 = \zeta_1 / (8\gamma_F)$ – hence dimensionless Q-tensor equation

$$\begin{aligned} \frac{\partial \mathbf{Q}}{\partial \tilde{t}} + \tilde{\mathbf{v}} \cdot \tilde{\nabla} \mathbf{Q} - \tilde{\Omega} \mathbf{Q} - \mathbf{Q} \tilde{\Omega} + \underbrace{\mathbf{Tu}}_{=(\zeta_2/\zeta_1)} \tilde{\mathbf{D}} \\ = \epsilon^2 \tilde{\nabla}^2 \mathbf{Q} + g_1(1-\theta) \mathbf{Q} + 3g_2 \mathbf{Q}^2 - \frac{1}{2} \text{tr}(\mathbf{Q}^2) \mathbf{Q} + \frac{1}{3} \mathbb{I} \left[\mathbf{Tu} \text{tr}(\tilde{\mathbf{D}}) - 3g_2 \text{tr}(\mathbf{Q}^2) \right], \end{aligned}$$

where

$$\alpha_F / (8\gamma_F) = -g_1 [1 - (T/T_*)] \equiv -g_1(1-\theta), \quad \beta_F / (8\gamma_F) = g_2, \quad \epsilon = k / (L^2 \gamma_F).$$

Hence also, a dimensionless momentum equation:

$$\frac{\partial \tilde{\mathbf{v}}}{\partial \tilde{t}} + \tilde{\mathbf{v}} \cdot \tilde{\nabla} \tilde{\mathbf{v}} = -\tilde{\nabla} \tilde{p} + \frac{1}{\text{Re}} \nabla \cdot \tilde{\mathbf{D}} + \text{Br} \nabla \cdot \left[-\epsilon^2 \tilde{\nabla} \mathbf{Q} \odot \tilde{\nabla} \mathbf{Q} + \dots \right],$$

Non-dimensional equations – dimensionless groups

Length scale L and timescale $t_0 = \zeta_1 / (8\gamma_F)$ – hence dimensionless Q-tensor equation

$$\begin{aligned} \frac{\partial \mathbf{Q}}{\partial \tilde{t}} + \tilde{\mathbf{v}} \cdot \tilde{\nabla} \mathbf{Q} - \tilde{\Omega} \mathbf{Q} - \mathbf{Q} \tilde{\Omega} + \underbrace{\mathbf{Tu}}_{=(\zeta_2/\zeta_1)} \tilde{\mathbf{D}} \\ = \epsilon^2 \tilde{\nabla}^2 \mathbf{Q} + g_1(1-\theta) \mathbf{Q} + 3g_2 \mathbf{Q}^2 - \frac{1}{2} \text{tr}(\mathbf{Q}^2) \mathbf{Q} + \frac{1}{3} \mathbb{I} \left[\mathbf{Tu} \text{tr}(\tilde{\mathbf{D}}) - 3g_2 \text{tr}(\mathbf{Q}^2) \right], \end{aligned}$$

where

$$\alpha_F / (8\gamma_F) = -g_1 [1 - (T/T_*)] \equiv -g_1(1-\theta), \quad \beta_F / (8\gamma_F) = g_2, \quad \epsilon = k / (L^2 \gamma_F).$$

Hence also, a dimensionless momentum equation:

$$\frac{\partial \tilde{\mathbf{v}}}{\partial \tilde{t}} + \tilde{\mathbf{v}} \cdot \tilde{\nabla} \tilde{\mathbf{v}} = -\tilde{\nabla} \tilde{p} + \frac{1}{\text{Re}} \nabla \cdot \tilde{\mathbf{D}} + \text{Br} \nabla \cdot \left[-\epsilon^2 \tilde{\nabla} \mathbf{Q} \odot \tilde{\nabla} \mathbf{Q} + \dots \right],$$

where

$$\text{Br} = \frac{\zeta_1}{\rho_0 L(L/t_0)}, \quad \text{Re} = \frac{\rho_0 L(L/t_0)}{\zeta_3}.$$

Limiting case

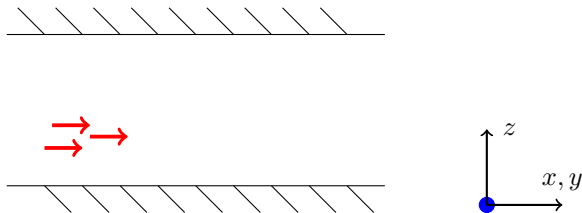
We work on the limit where $\text{Br} = 0$ – no feedback of Q-tensor gradients into the flow – flow is independent of Q-tensor. We can therefore apply **standard chaotic flows** to the Q-tensor dynamics

$$\begin{aligned} \frac{\partial \mathbf{Q}}{\partial \tilde{t}} + \tilde{\mathbf{v}} \cdot \tilde{\nabla} \mathbf{Q} - \tilde{\boldsymbol{\Omega}} \mathbf{Q} - \mathbf{Q} \tilde{\boldsymbol{\Omega}} + \underbrace{\text{Tu}}_{=(\zeta_2/\zeta_1)} \tilde{\mathbf{D}} \\ = \epsilon^2 \tilde{\nabla}^2 \mathbf{Q} + g_1(1 - \theta) \mathbf{Q} + 3g_2 \mathbf{Q}^2 - \frac{1}{2} \text{tr}(\mathbf{Q}^2) \mathbf{Q} + \frac{1}{3} \mathbb{I} \left[\text{Tu} \text{tr}(\tilde{\mathbf{D}}) - 3g_2 \text{tr}(\mathbf{Q}^2) \right], \end{aligned}$$

The **flow timescales** and the **tumbling parameter** Tu are the key parameters.

Two-dimensional geometry I

We work with a sample confined between two narrowly separated parallel plates. **Anchoring conditions** are applied in the same fashion at the top and bottom walls such that the director is parallel to the plates.



As such, the Q-tensor simplifies:

$$\mathbf{Q} = \begin{pmatrix} q & r & 0 \\ r & s & 0 \\ 0 & 0 & -(q + s) \end{pmatrix}.$$

Two-dimensional geometry II

The dynamical equations for the Q-tensor also simplify – and we only have three of them:

$$\begin{aligned}\frac{\partial q}{\partial t} + \mathbf{v} \cdot \nabla q - 2\Omega_{12}r &= \epsilon^2 \nabla^2 q \\ &+ g_1(1 - \theta)q + 3g_2(q^2 + r^2) - (q^2 + r^2 + s^2 + qs)q - 2g_2(q^2 + r^2 + s^2 + qs), \\ \frac{\partial r}{\partial t} + \mathbf{v} \cdot \nabla r - \Omega_{12}(s - q) + \text{Tu}D_{12} &= \epsilon^2 \nabla^2 r \\ &+ g_1(1 - \theta)r + 3g_2(q + s)r - (q^2 + r^2 + s^2 + qs)r, \\ \frac{\partial s}{\partial t} + \mathbf{v} \cdot \nabla s + 2\Omega_{12}r &= \epsilon^2 \nabla^2 s \\ &+ g_1(1 - \theta)s + 3g_2(r^2 + s^2) - (q^2 + r^2 + s^2 + qs)s - 2g_2(q^2 + r^2 + s^2 + qs),\end{aligned}$$

Fixed-point analysis

We look at fixed points for $\mathbf{v} = \nabla = \partial_t = 0$. Remarkably, all fixed points can be found in closed form and categorized:

- Type 1: $r = 0$ and $q = as$, where $a = 1$, $a = -2$, or $a = -1/2$, and

$$s = -g_2 \left(1 - \frac{3}{2} \frac{1}{1+a+a^2} \right) \pm \sqrt{g_2^2 \left(1 - \frac{3}{2} \frac{1}{1+a+a^2} \right)^2 + \frac{g_1(1-\theta)}{1+a+a^2}}.$$

For $a = 1$, $s = A_{\pm} - g_2$, where

$$A_{\pm} = \frac{1}{2}g_2 \pm \sqrt{\frac{1}{4}g_2^2 + \frac{1}{3}g_1(1-\theta)}$$

Fixed-point analysis

We look at fixed points for $\mathbf{v} = \nabla = \partial_t = 0$. Remarkably, all fixed points can be found in closed form and categorized:

- Type 1: $r = 0$ and $q = as$, where $a = 1$, $a = -2$, or $a = -1/2$, and

$$s = -g_2 \left(1 - \frac{3}{2} \frac{1}{1+a+a^2} \right) \pm \sqrt{g_2^2 \left(1 - \frac{3}{2} \frac{1}{1+a+a^2} \right)^2 + \frac{g_1(1-\theta)}{1+a+a^2}}.$$

For $a = 1$, $s = A_{\pm} - g_2$, where

$$A_{\pm} = \frac{1}{2}g_2 \pm \sqrt{\frac{1}{4}g_2^2 + \frac{1}{3}g_1(1-\theta)}$$

- Type 2: $r \neq 0$, q = arbitrary, and $s = -q + A_{\pm}$, with

$$r^2 = g_1(1-\theta) + 3g_2A_{\pm} - A_{\pm}^2 + A_{\pm}q - q^2.$$

This gives the critical temperature: a liquid-crystal phase if r^2 is real, hence $\theta \leq \theta_c$, where

$$\theta_c = \frac{3}{4} \frac{g_2^2}{g_1} + 1.$$

Fixed points – stability

Using standard eigenvalue analysis,

- Case 1a ($r = 0, s = q$) gives stable and unstable states – **biaxial**
- Case 1b,c ($r = 0, s \neq q$) give neutral and unstable state – **uniaxial**
- Case 2 gives neutral and unstable state – **uniaxial**

Fixed points – stability

Using standard eigenvalue analysis,

- Case 1a ($r = 0, s = q$) gives stable and unstable states – **biaxial**
- Case 1b,c ($r = 0, s \neq q$) give neutral and unstable state – **uniaxial**
- Case 2 gives neutral and unstable state – **uniaxial**

Another possibility (Case 3)– $s(t) = \lambda q(t)$, where $\lambda = \text{Const.}$. Dynamics collapse into a single equation

$$\frac{dq}{dt} = \Phi(q), \quad r^2 = (2\lambda^2 + 5\lambda + 2)q^2$$

This gives more uniaxial fixed points $q_0 = A_{\pm}(1 + \lambda)^{-1}$, which are all stable, as $\Phi'(q_0) \leq 0$.

Case 3 fixed points agree with Case 1b,c and Case 2 fixed points yet Case 3 is stable while the others are not – Case 3 is a restriction of other cases along **stable eigendirections**.

Numerics without flow

To understand evolution, we study Q-tensor dynamics (three-equation model) in the absence of flow using a pseudospectral numerical method on a doubly-periodic spatial domain. Two sets of initial conditions considered:

- Uni-axial initial conditions $\hat{n} = (\cos \varphi, \sin \varphi)$, with a different random number φ and a different random value of the scalar order parameter S at each point in space:

$$\mathbf{Q}(t=0) = \mathbf{Q} = \frac{1}{2}S \begin{pmatrix} \cos^2 \varphi - 1/3 & \cos \varphi \sin \varphi & 0 \\ \cos \varphi \sin \varphi & \sin^2 \varphi - 1/3 & 0 \\ 0 & 0 & -1/3 \end{pmatrix}$$

- Bi-axial initial conditions, with

$$\mathbf{Q}(t=0) = \begin{pmatrix} \lambda_1 n_x^2 + \lambda_2 n_y^2 & (\lambda_1 - \lambda_2) n_x n_y & 0 \\ (\lambda_1 - \lambda_2) n_x n_y & \lambda_1 n_y^2 + \lambda_2 n_x^2 & 0 \\ 0 & 0 & -(\lambda_1 + \lambda_2) \end{pmatrix}$$

with λ_1 and λ_2 drawn from uniform distributions such that $\text{tr}[\mathbf{Q}(t=0)] = 0$.

Results – Uniaxial initial conditions

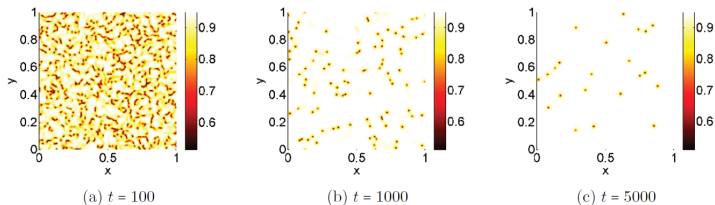


FIG. 1. Snapshots of scalar order parameter at various times.

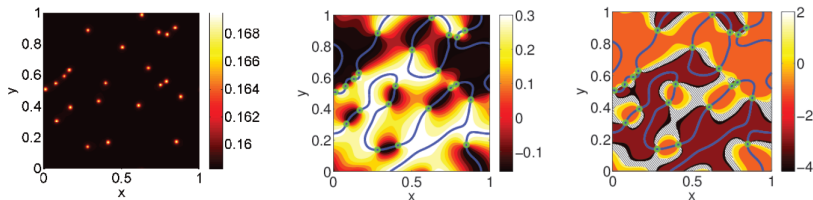
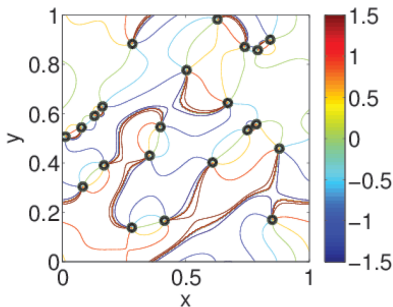


FIG. 2. Fuller characterization of the system at $t = 5,000$. (a) Plot of $s + q$ at $t = 5000$ revealing a bimodal distribution. The value $s + q \approx A_+$ corresponds to a type-3 stable fixed point while the $s + q \approx 2(A_+ - g_2)$ corresponds to a type-1(a) unstable bi-axial fixed point; (b) Plot of s at the same time. The small circular contours correspond $s + q \approx 2(A_+ - g_2)$ (i.e. bi-axial regions) and the larger contours correspond to $r = 0$; (c) Plot of $\lambda = s/q$ for $|q| > 0.05$ (the hatched regions correspond to $|q| < 0.05$).

Defects

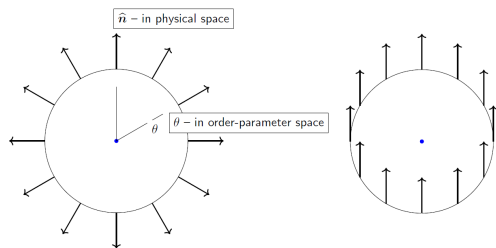
Why do unstable biaxial fixed points persist at late times?

- Answer is due to defects – director $\hat{n} = (\cos \varphi, \sin \varphi)$ experiences jumps in φ (line defects).
- Line defects end at defect **cores**, which coincide with biaxial islands.
- Each defect core has a topological charge (winding number) $\pm 1/2$.
- Total topological charge is conserved, meaning biaxial islands can't spontaneously disappear – they have to **merge**, thereby gradually reducing system energy.



Aside – topological theory of defects

- The director \hat{n} is a unit vector in two dimensions, so it corresponds to the topological space $G = SO(2)$
- Identifying both ends of the director (isotropy subgroup H) tells us that the relevant topological space is in fact $R = G/H = \mathbb{R}P^1$ – **order-parameter space**

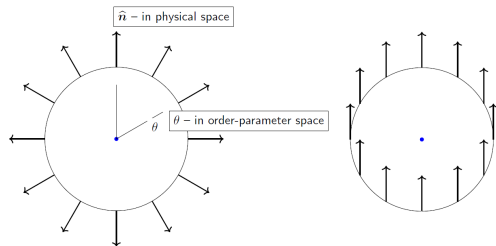


The two distinct scenarios for a vector field \hat{n} surrounding a point, with $|\hat{n}| = 1$.

Aside – topological theory of defects

- The director \hat{n} is a unit vector in two dimensions, so it corresponds to the topological space $G = SO(2)$
- Identifying both ends of the director (isotropy subgroup H) tells us that the relevant topological space is in fact $R = G/H = \mathbb{R}P^1$ – **order-parameter space**
- Theory tells us that the fundamental group (and the higher homotopy groups) of the order-parameter space classifies defects, in particular:

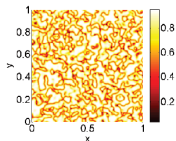
Point defects in 2D correspond to π_1 . We have $\pi_1(\mathbb{R}P^1) = \mathbb{Z}/2$, so infinitely many classes of point defects. Half-integers correspond to line defects, integer values correspond to **radial hedgehogs**.



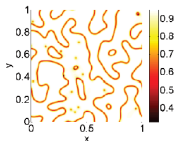
The two distinct scenarios for a vector field \hat{n} surrounding a point, with $|\hat{n}| = 1$.

Results – Biaxial initial conditions

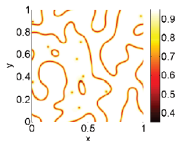
The system forms domains – pure stable biaxial fixed points or mixed domains containing uniaxial fixed points and unstable biaxial islands:



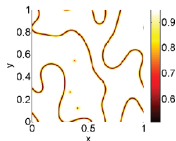
(a) $t = 100$



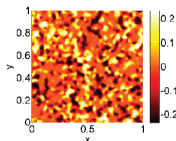
(b) $t = 1000$



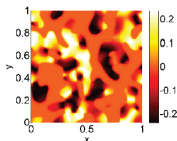
(c) $t = 2000$



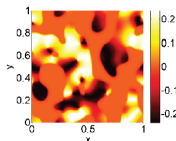
(d) $t = 5000$



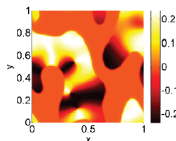
(e) $t = 100$



(f) $t = 1000$



(g) $t = 2000$



(h) $t = 5000$

Top: snapshots of scalar order parameter at various times for the bi-axial initial data.
Bottom: corresponding snapshots for r . The domains with $r = 0$ correspond to the bi-axial state.

Coarsening

Simulations show that system self-orders over time – random initial conditions coalesce into domains.

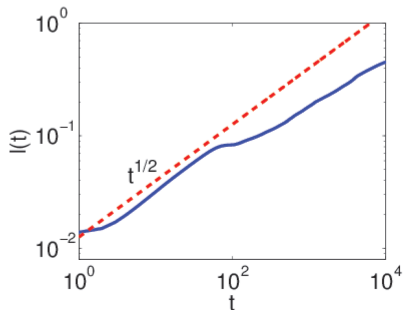
Quantified by measuring

$$L(t) = 2\pi/k_1, \quad k_1 = \frac{\int |\widehat{C}_{\mathbf{k}}|^2 d^2k}{\int |\mathbf{k}|^{-1} |\widehat{C}_{\mathbf{k}}|^2 d^2k},$$

where

$$\langle \mathcal{S} \rangle = \frac{1}{|\Omega|} \int_{\Omega} \mathcal{S}(\mathbf{x}) d^2x,$$

$$\widehat{C}_{\mathbf{k}} = \int_{\Omega} e^{-i\mathbf{x}\cdot\mathbf{k}} (\mathcal{S} - \langle \mathcal{S} \rangle) d^2x.$$



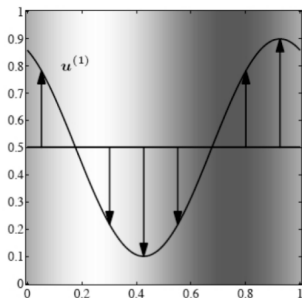
Calculation shows $L(t) \sim t^{1/2}$
– **diffusive scaling**

Not the same L as before – sorry!

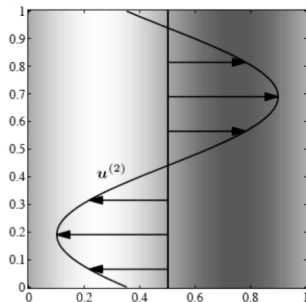
Model sine flow

The effect of chaotic shear flow via passive advection is first modelled using the following quasi-periodic random-phase sine flow with period τ : at time t , the velocity field is given by

$$\begin{aligned}u &= A \sin(k_0 y), & 0 \leq \text{mod}(t, \tau) < \frac{1}{2}\tau, \\v &= A \sin(k_0 x), & \frac{1}{2}\tau \leq \text{mod}(t, \tau) < \tau,\end{aligned}$$



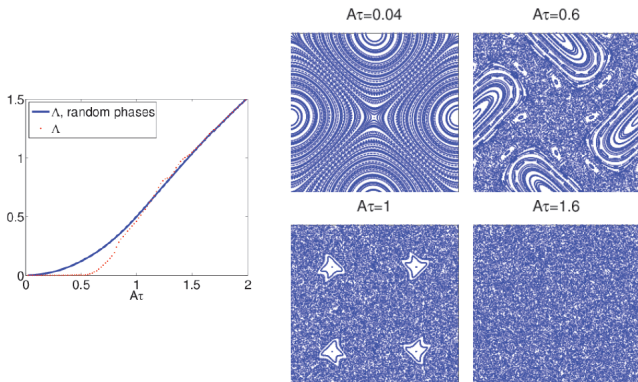
(a) First half-period



(b) Second half-period

Schematic description of the sine flow in each quasi-period.

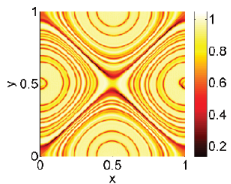
Chaoticness is quantified using the average Lyapunov exponent



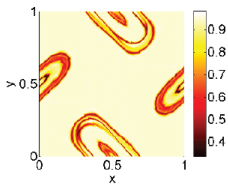
(Left) The average Lyapunov exponent for the sine flow (dotted line).

Shown for comparison is the average Lyapunov exponent for a similar sine flow wherein the u - and v - phases are renewed with separate independent random values once per flow period τ . (Right) Lagrangian trajectories for the sine flow. Regular regions are visible where the trajectories are periodic. As $A\tau$ increases the regular regions decrease such that by $A\tau = 1.6$ the entire flow domain possesses chaotic trajectories. The horizontal axis is the x -axis and the vertical axis is the y -axis. The coordinates range from $(x, y) = 0$ in the bottom left-hand corner to $(x, y) = (1, 1)$ in the top right-hand corner.

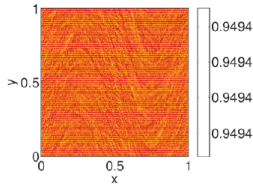
Results – no tumbling



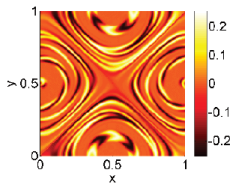
(a) $A\tau = 0.04$



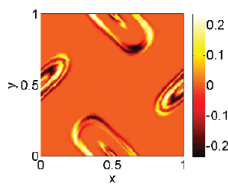
(b) $A\tau = 0.6$



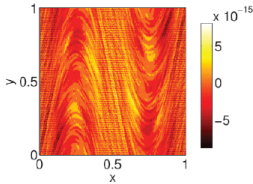
(c) $A\tau = 1.6$



(d) $A\tau = 0.04$



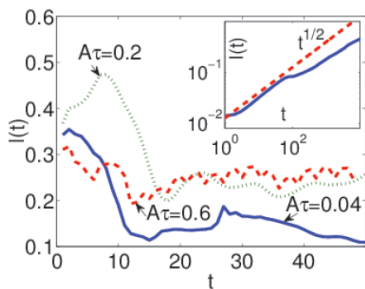
(e) $A\tau = 0.6$



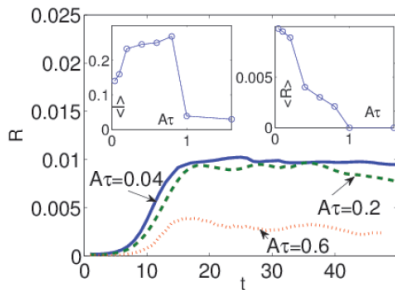
(f) $A\tau = 1.6$

Across the top: snapshots of scalar order parameter at various times for various values of $A\tau$, with $Tu = 0$. Across the bottom: corresponding snapshots of r . Snapshots in the first two columns are taken at $t = 320$. The third column (figures (c) and (f)) concerns $A\tau = 1.6$, for which the snapshots are taken at $t = 320$; these are included here to demonstrate the relaxation to a uniform state for the large values of $A\tau$. The compressed colour bars in these figures is a consequence of the rapid relaxation to the uniform steady state.

Coarsening is arrested



(a)



(b)

(a) Time evolution of the domain scale $L(t)$ for various values of $A\tau$. The inset shows the time-averaged values of $L(t)$ for a much larger range of $A\tau$ -values, with angle brackets denoting a time average. The time-averages are taken over intervals where the Q -tensor dynamics are in a statistically steady state. (b) The same, for $R := L_x^{-1} L_y^{-1} \iint r^2 dx dy$

Theoretical explanation of the different regimes I

Summarizing,

- For small $A\tau$ the domain structure persists – biaxial domains and mixed domains, ‘frozen in’ by the flow structure
- For larger values of $A\tau$ the domains shrink, leaving islands in a sea of biaxial
- For the largest values of $A\tau$ the solution relaxes globally to the biaxial fixed point

Reason: Diffusion is small, so along Lagrangian trajectories, we can write

$$\frac{d}{dt} \begin{pmatrix} q \\ r \\ s \end{pmatrix} = \begin{pmatrix} F_1(q, r, s) \\ F_2(q, r, s) \\ F_3(q, r, s) \end{pmatrix} + \begin{pmatrix} 2r\Omega_{12} \\ \Omega_{12}(s - q) \\ -2r\Omega_{12} \end{pmatrix}, \quad \text{Tu} = 0.$$

where $(F_1, F_2, F_3)^T$ encode the Q -tensor dynamics, and where d/dt is the Lagrangian derivative along particle trajectories.

Theoretical explanation of the different regimes II

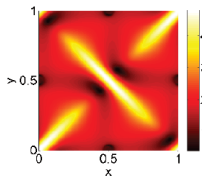
... along Lagrangian trajectories,

$$\frac{d}{dt} \begin{pmatrix} q \\ r \\ s \end{pmatrix} = \begin{pmatrix} F_1(q, r, s) \\ F_2(q, r, s) \\ F_3(q, r, s) \end{pmatrix} + \begin{pmatrix} 2r\Omega_{12} \\ \Omega_{12}(s - q) \\ -2r\Omega_{12} \end{pmatrix}, \quad \text{Tu} = 0.$$

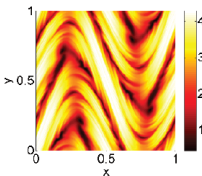
- $\Omega_{12} \neq 0$ means that uniaxial fixed points are no longer a solution – but the biaxial one persists – hence biaxial fixed point is naturally selected.
- But for $\tau \rightarrow 0$ (specifically, $A\tau \ll 1$) Ω_{12} oscillates rapidly along a Lagrangian trajectory, meaning it can be replaced by its average value – which is zero.
- So along such trajectories, for $A\tau \ll 1$, $\Omega_{12} \rightarrow 0$, meaning that all fixed points are supported, hence mixed domains are possible.
- Explains previous findings at low values of $A\tau$; robust to details of flow structure (same conclusions for other model flows).

Results with tumbling

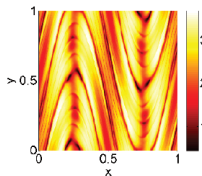
Tumbling adds an inhomogeneity ('source term') to the Q -tensor equations, driving system out of equilibrium.



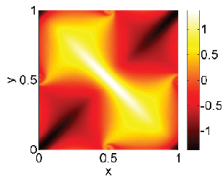
(a) $Ar\tau = 0.04$



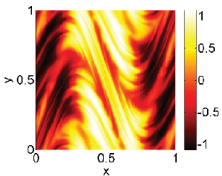
(b) $Ar\tau = 0.8$



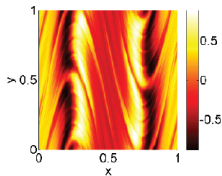
(c) $Ar\tau = 1.6$



(d) $Ar\tau = 0.04$



(e) $Ar\tau = 0.8$



(f) $Ar\tau = 1.6$

Across the top: snapshots of scalar order parameter at various times for various values of Ar , with $Tu = 1$. Across the bottom: corresponding snapshots of r . The snapshots are illustrative and are taken at different times: the snapshots at $Ar\tau = 0.04, 0.8, 1.6$ are taken at $t = 120, 200, 6$ respectively.

Discussion and Conclusions

- We have formulated a theory for flow and liquid-crystal dynamics in a planar system.

Discussion and Conclusions

- We have formulated a theory for flow and liquid-crystal dynamics in a planar system.
- No backreaction – **passive advection**

Discussion and Conclusions

- We have formulated a theory for flow and liquid-crystal dynamics in a planar system.
- No backreaction – **passive advection**
- Identified fixed points and their stability analytically

Discussion and Conclusions

- We have formulated a theory for flow and liquid-crystal dynamics in a planar system.
- No backreaction – **passive advection**
- Identified fixed points and their stability analytically
- For a chaotic flow without tumbling, the fixed points determine the result, with rapidly-varying flows admitting a variety of fixed points (slowly-varying flows only admit the biaxial one)

Discussion and Conclusions

- We have formulated a theory for flow and liquid-crystal dynamics in a planar system.
- No backreaction – **passive advection**
- Identified fixed points and their stability analytically
- For a chaotic flow without tumbling, the fixed points determine the result, with rapidly-varying flows admitting a variety of fixed points (slowly-varying flows only admit the biaxial one)
- With tumbling, Q -tensor morphology follows the flow (source term)

Discussion and Conclusions

- We have formulated a theory for flow and liquid-crystal dynamics in a planar system.
- No backreaction – **passive advection**
- Identified fixed points and their stability analytically
- For a chaotic flow without tumbling, the fixed points determine the result, with rapidly-varying flows admitting a variety of fixed points (slowly-varying flows only admit the biaxial one)
- With tumbling, Q -tensor morphology follows the flow (source term)
- These insights provide ways of controlling the morphology with stirring

Discussion and Conclusions

- We have formulated a theory for flow and liquid-crystal dynamics in a planar system.
- No backreaction – **passive advection**
- Identified fixed points and their stability analytically
- For a chaotic flow without tumbling, the fixed points determine the result, with rapidly-varying flows admitting a variety of fixed points (slowly-varying flows only admit the biaxial one)
- With tumbling, Q -tensor morphology follows the flow (source term)
- These insights provide ways of controlling the morphology with stirring
- Future work – investigate robustness of results to different model flows

Discussion and Conclusions

- We have formulated a theory for flow and liquid-crystal dynamics in a planar system.
- No backreaction – **passive advection**
- Identified fixed points and their stability analytically
- For a chaotic flow without tumbling, the fixed points determine the result, with rapidly-varying flows admitting a variety of fixed points (slowly-varying flows only admit the biaxial one)
- With tumbling, Q -tensor morphology follows the flow (source term)
- These insights provide ways of controlling the morphology with stirring
- Future work – investigate robustness of results to different model flows
- Apply known techniques to the reduced planar model:
 - ▶ Bounds and *a priori* estimates
 - ▶ Lubrication theory
 - ▶ DNS of the fully coupled system – **the backreaction will be back!**